



## OPEN ACCESS

## EDITED BY

Chong Xu,  
Ministry of Emergency Management, China

## REVIEWED BY

Yankun Wang,  
Yangtze University, China  
Ryszard Hejmanowski,  
AGH University of Science and Technology,  
Poland

## \*CORRESPONDENCE

Shaomin Liu,  
✉ liusm2023@126.com  
Mingzhou Bai,  
✉ 279459260@qq.com

RECEIVED 17 January 2024

ACCEPTED 28 February 2024

PUBLISHED 11 March 2024

## CITATION

Liu S and Bai M (2024), Land subsidence along the Beijing-Tianjin high-speed railway before and after the South-to-North water diversion project with multi-source monitoring datasets.

*Front. Earth Sci.* 12:1372105.  
doi: 10.3389/feart.2024.1372105

## COPYRIGHT

© 2024 Liu and Bai. This is an open-access article distributed under the terms of the [Creative Commons Attribution License \(CC BY\)](https://creativecommons.org/licenses/by/4.0/). The use, distribution or reproduction in other forums is permitted, provided the original author(s) and the copyright owner(s) are credited and that the original publication in this journal is cited, in accordance with accepted academic practice. No use, distribution or reproduction is permitted which does not comply with these terms.

# Land subsidence along the Beijing-Tianjin high-speed railway before and after the South-to-North water diversion project with multi-source monitoring datasets

Shaomin Liu<sup>1,2,3\*</sup> and Mingzhou Bai<sup>1,2\*</sup>

<sup>1</sup>School of Civil Engineering, Beijing Jiaotong University, Beijing, China, <sup>2</sup>Beijing Urban Rail Transit Safety and Disaster Prevention Engineering and Technology Research Center, Beijing, China, <sup>3</sup>Beijing Institute of Geology and Mineral Exploration, Beijing, China

The development of land subsidence has seriously affected the safe operation of Beijing-Tianjin high-speed railway. The South-to-North Water Diversion Project Central Route (SNWDP-CR) was officially put into operation in December 2014. It has changed the water supply pattern in Beijing and provided conditions for reducing groundwater exploitation and controlling land subsidence. In this paper, the time-series interferometric data, *in situ* monitoring data of recent 20 years and the basic geological datasets are combined to compare and analyze the changes of groundwater level, land subsidence and the main subsidence layers along the Beijing-Tianjin high-speed railway before and after the SNWDP-CR. The effects of the environment of Quaternary sedimentary, groundwater exploitation and soil deformation of different lithology on land subsidence along the high-speed railway under the background of new water conditions are revealed. The main conclusions are as follows: 1) The serious land subsidence area along the Beijing-Tianjin high-speed railway always concentrated in the section of DK11-DK23. After the operation of SNWDP-CR, the land subsidence along the railway generally showed a slowing trend. The maximum subsidence rate was reduced from 80 mm/yr to 49 mm/yr. The length of subsidence rate that more than 50 mm/yr of the section was reduced from 8.0 km to 0 km. 2) The groundwater level of different aquifer groups along the Beijing-Tianjin high-speed railway rose and declined before and after the SNWDP-CR. In eastern part of the plain, the groundwater level of each aquifer group has changed from a continuous decline (range 0.13–1.82 m) to a gradual rise (range 0.45–1.87 m) since 2017. However, in the southeast of the plain, the groundwater level still showed a continuous decline trend, with an average annual decline of 1.2–1.8 m. 3) From 2006 to 2019, the subsidence of the first, second and third compression layer group along the railway accounted for 2.71%, 28.29% and 69%, respectively. The third compression layer group (monitoring layer 94–182 m) had the largest subsidence proportion and was the main subsidence layer. 4) The land subsidence along the Beijing-Tianjin high-speed railway is controlled by the basement structure. The difference of groundwater exploitation intensity led to differences in the spatial distribution of land subsidence along the railway.

The subsidence of the soil layer below the bearing layer (about 50 m) of the high-speed railway pile foundation exhibited the characteristics of viscoplastic or viscoelastic plasticity deformation. This section of strata is a key layer that needs to be considered for land subsidence control along the Beijing-Tianjin high-speed railway in the future.

#### KEYWORDS

land subsidence, high-speed railway, water diversion project, groundwater level, soil deformation characteristics

## 1 Introduction

The high-speed railway operation networks with speeds of over 300 km per hour have been established in Japan, Europe, and North America (Hwang et al., 2008). Since the completion of the Beijing-Tianjin high-speed railway in 2008, multiple high-speed railways have been built and put into operation in China. The high-speed railways have very strict requirements for the stability, deformation degree, and smoothness of the foundation (Leng, 2011). When the first high-speed railway (Tokaido Shinkansen) has been built in Japan, due to insufficient attention to land subsidence, the uneven subsidence occurred on the railway track after its opening in 1964, resulting in a decrease in the maximum speed of the railway from 210 km/h to 160 km/h, and even to 90–100 km/h (Zhang, 1998). The Merced to SanJose section of the California High Speed Railway (CHSRA) in the United States was rerouted due to land subsidence in the E1 Nido area of the SanJoaquin. Uneven subsidence in the Picacho area of Arizona has affected the construction of the South Pacific Railway. The annual subsidence of Yunlin and Zhanghua in Taiwan, China has reached 7–8 cm, which has seriously threatened the safe operation of Taiwan's high-speed railway. If the subsidence not effectively alleviated, the service life of high-speed railway will only be 10 years (Hwang et al., 2008; Yang, 2013). In addition, high-speed railways in areas such as Tokyo in Japan (Zhang, 1998), Naole in Italy, Lisbon in Portugal (Heleno et al., 2013), Melia in Greece (Kontogianni et al., 2006), and Indonesia (Abidin et al., 2015; Li et al., 2019) have also been affected by uneven subsidence, and some sections have seriously affected the safe operation of high-speed railways. There are serious uneven subsidence issues along the maglev of Shanghai, the high-speed railway of Beijing-Tianjin, Beijing-Shanghai, and Datong-Xi'an, China (Hu et al., 2011; Jiang et al., 2013; Wang et al., 2014; Yang et al., 2020).

The Beijing-Tianjin high-speed railway is the first high-speed railway built in China. It began operation in 2008, with a design speed of 350 km/h. The entire line adopts ballastless tracks, and the length of the bridge foundation accounts for 87.7% of the total length of the line (Sun et al., 2009). The Beijing-Tianjin high-speed railway, as an important transportation artery for the "Beijing Tianjin integration strategy", passes through multiple major subsidence funnel areas in Beijing and Tianjin. The Beijing section of the high-speed railway passes through two major subsidence centers, Dongbalizhuang in Chaoyang District and Taihu in Tongzhou District (Li et al., 2007; Ge et al., 2010). In 2020, the maximum cumulative subsidence along the railway reached 1.6 m, with a historical maximum subsidence rate of 9 cm/yr. Moreover, there are multiple areas with significant differential subsidence at the edge of the subsidence funnel (Lei et al., 2020). The maximum

differential subsidence near Kanghua Bridge, where the Beijing-Tianjin high-speed railway intersects with the Fifth Ring Road, reached 5.5 cm, resulting in a corner loss of 1/1,400 (Liu et al., 2016). At present, some disposal measures have been adopted in this region, such as adjusting bearings, compensating for elevation loss, and reducing speed. These measures can only ensure the safety of the railway in the near future, but the differential subsidence cannot be ignored in the medium and long term impact of high-speed railway. According to the subsidence control regulations in the high-speed railway design specifications of China, the uniform subsidence of bridge foundations should be controlled within 20 cm, the differential subsidence between adjacent bridge foundations should be controlled within 5 cm, and the corner loss caused by uneven subsidence should not exceed 1/1,000. The slope and smoothness of the Beijing-Tianjin high-speed railway are severely affected by differential subsidence. If differential subsidence cannot be effectively prevented and controlled, the service life of the Beijing-Tianjin high-speed railway will be significantly reduced (Zhao et al., 2020).

In December 2014, the South-to-North Water Diversion Project Central Route (SNWDP-CR) was completed, and the Yangtze River water was diverted into Beijing. The South-to-North Water Diversion Project (SNWDP) is the largest water control project which has ever been built, and the aim of which is to optimize the reallocation of water resources from South China to North China (Bai and Liu, 2018). The SNWDP-CR diverts water from the Danjiangkou reservoir (32° 43' North, 111° 34' East) on the Han River via artificial canals that cross Henan and Hebei Provinces to the Tuancheng Lake of Beijing (39° 55' North, 116° 24' East). From 2014 to 2020, a total of over  $6.0 \times 10^8 \text{ m}^3$  of water from the SNWDP diverted into Beijing, with approximately  $4.0 \times 10^8 \text{ m}^3$  used for urban water supply,  $8.0 \times 10^8 \text{ m}^3$  stored in large and medium-sized reservoirs, and  $1.2 \times 10^8 \text{ m}^3$  used for groundwater recharge. At the same time, a series of measures such as groundwater reduction and recharge has been implemented in Beijing. The exploitation of groundwater has been decreased year by year, from  $19.6 \times 10^8 \text{ m}^3$  in 2014 decreased to  $13.5 \times 10^8 \text{ m}^3$  in 2020. In addition, from 2015 to 2018, the precipitation in Beijing was relatively abundant. The average annual precipitation was 619.0 mm, which was 49.0 mm higher than the average annual precipitation. Therefore, under the comprehensive influence of various factors mentioned above, the average groundwater level in the plain of Beijing has rebounded by 3.6 m (Bulletin of Beijing Water Resources, 2020). During this period, the land subsidence rate in Beijing gradually decreased, and the land subsidence along the Beijing-Tianjin high-speed railway also showed a slowing trend. Related research showed that the

maximum subsidence rate along the Beijing-Tianjin high-speed railway in 2020 was 56.0 mm/yr (Lei et al., 2020).

At present, some scholars have carried out abundant research on the distribution characteristics of land subsidence along high-speed railways. Li et al. (2019) analyzed the land subsidence and its influencing factors along the Jakarta-Bandung high-speed railway in Indonesia. The development trend of land subsidence in main road sections was predicted by numerical simulation technology, and relevant countermeasures were put forward. Hwang et al. (2008) used GPS and leveling technology to monitor the land subsidence along the high-speed railway in Yunlin and Changhua areas of Taiwan, China. Hu et al. (2011) adopted Synthetic Aperture Radar Interferometry (InSAR) and numerical simulation techniques to analyze the changes and future development trend of groundwater and land subsidence along the Beijing-Shanghai high-speed railway. Shi et al. (2019) and Chen et al. (2021) used InSAR technology to monitor the distribution characteristics of land subsidence along the Beijing-Tianjin high-speed railway. At the same time, combined with geological conditions, the causes of land subsidence were analyzed comprehensively. In addition, some scholars have studied the temporal and spatial distribution characteristics and the changes of land subsidence along the Beijing-Tianjin high-speed railway before and after the SNWDP-CR (Ge et al., 2010; Shi et al., 2014; Zhang et al., 2014; Duan et al., 2016; Zhang et al., 2019; Zhao et al., 2020; Chen et al., 2020; Lu et al., 2023). With water supply of the SNWDP-CR, the water situation has significantly changed in Beijing, and the groundwater level has changed from declining to rising in many areas. However, there is limited research on the comprehensive analysis of groundwater level, land subsidence, soil deformation characteristics, and influencing factors along the Beijing-Tianjin high-speed railway before and after the SNWDP-CR with multi-source monitoring datasets. In this paper, the time-series InSAR monitoring data, *in situ* monitoring data of recent 20 years (such as groundwater level data, groundwater exploitation data and extensometer data) and a variety of basic geological data sets were combined to compare and analyze the changes of groundwater level, land subsidence and the main subsidence layers along the Beijing-Tianjin high-speed Railway before and after the SNWDP-CR. The effects of the environment of Quaternary sedimentary, groundwater exploitation and soil deformation of different lithology on land subsidence along the high-speed railway under the background of new water conditions were studied. The results can provide a basis for the safe operation and subsidence prevention of high-speed railways.

## 2 Geological condition

The total length of Beijing-Tianjin high-speed railway (Beijing section) is about 50 km, from Beijing South Station to Yongledian in Tongzhou District. The terrain along the high-speed railway slopes from northwest to southeast, with a slope of about 1%. The concealed faults that the Beijing-Tianjin high-speed railway passes through include the Nanyuan-Tongzhou Fault and Xiadian-Mafang Fault. The maximum difference in thickness of the Quaternary system on both sides of the fault is several hundred meters. In terms of hydrogeological units, the Beijing-Tianjin high-speed railway (Beijing section) is located in the middle and lower part

of the Yongding River alluvial-proluvial plain. The thickness of the Quaternary system along the railway is influenced by the basement structure, gradually increasing from northwest to southeast, with more layers and the particles gradually changing from coarse to fine. The lithology is that sand, gravel, and cohesive soil layers appear alternately, and the cohesive soil is dominant (Lei et al., 2022) (Figure 1).

Corresponding to the sedimentary characteristics of the Quaternary, the aquifer system along the high-speed railway can be vertically divided into three main aquifer groups. The first aquifer system (unconfined aquifer and shallow confined aquifer) includes the Quaternary Holocene ( $Q_4$ ) and upper Pleistocene ( $Q_3$ ) alluvial deposits, the bottoms of which are at depths of about 25 m and 80–120 m respectively. The second aquifer system (medium-deep confined aquifers) is a multilayered structure of the Quaternary middle Pleistocene ( $Q_2$ ) strata, the lithology of which is mainly medium-coarse sand, partly with gravel, and the bottom depth of which is about 180 m. The third aquifer system (deep confined aquifers) is the lower Pleistocene ( $Q_1$ ) stratum of the Quaternary system with a multilayer structure, which is dominated by medium-coarse sand and gravel, the bottom boundary of which is the Quaternary basement at about 260–300 m depth (Lei et al., 2016; Lei et al., 2023) (Figure 2).

Corresponding to the division of Quaternary compression layer groups, the soil layers along the high-speed railway can be divided into three main compression layer groups. The first compression group ( $Q_4+Q_3$ ) is widely distributed in the Beijing plain, the lithology of which is Holocene or upper Pleistocene alluvial facies, alluvial silt, and cohesive soil, and the bottom depth of which is less than 100 m. The soil layers are mostly of normal consolidation or micro-overconsolidation, plastic, and have moderate compressibility. The second compression group ( $Q_2$ ) is mainly distributed in the middle and lower parts of the alluvial-proluvial plain of Beijing, the lithology of which is silt, silty clay, and clay of the middle Pleistocene alluvial and alluvial lacustrine deposits and the bottom depth of which is 150–180 m. Most of the soil layers are normally consolidated, plastic, and have medium or low compressibility. The third compression group ( $Q_1$ ) is mainly distributed in the center of several major subsidence depressions. The lithology is silty clay and clay of the lower Pleistocene river and lake facies, whose bottom depth is about 260–300 m or is the bottom of the Quaternary. The soil layers are mostly of normal consolidation or overconsolidation, plastic or hard plastic, low compressibility, and most of them are in a hard state (Lei et al., 2016; Lei et al., 2023) (Figure 2).

## 3 Data set and methodology

### 3.1 Data set

In this paper, the changes of groundwater level, land subsidence and the main subsidence layers along the Beijing-Tianjin high-speed railway before and after the SNWDP-CR were analyzed with multi-source monitoring datasets, and the effects of the environment of Quaternary sedimentary, groundwater exploitation and soil deformation of different lithology on land subsidence along the high-speed railway under the background of new water conditions

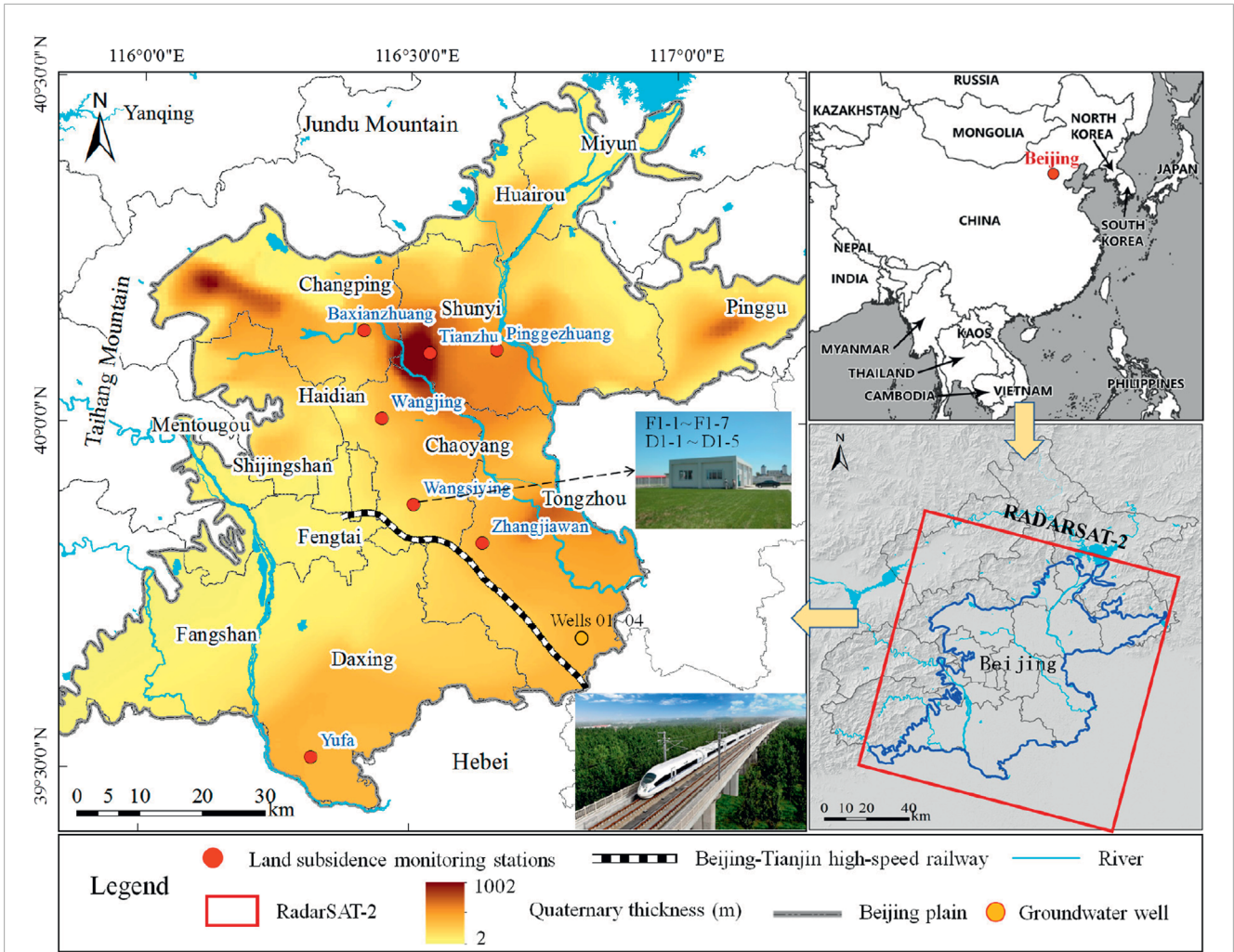


FIGURE 1 The location of Beijing-Tianjin high-speed railway and the thickness of Quaternary. The position of land subsidence monitoring stations and the range of RadarSAT-2 data are provided.

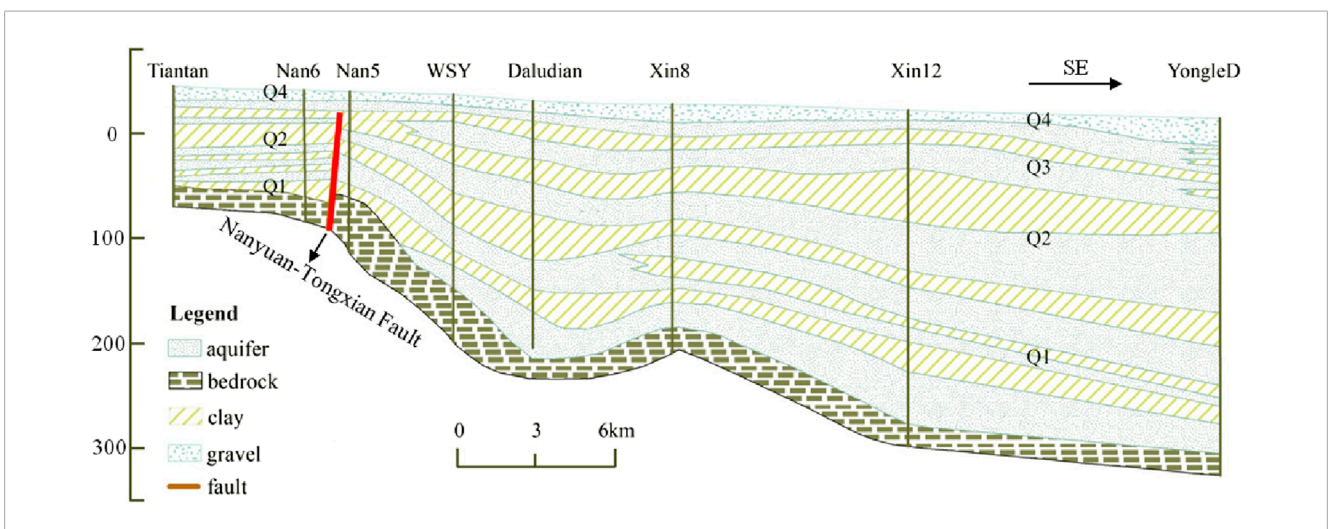


FIGURE 2 Hydrogeological cross-section along the Beijing-Tianjin high-speed railway.

TABLE 1 Acquisition parameters of Radarsat-2 datasets.

SAR sensor	Radarsat-2
Orbit direction	Descending
Orbit altitude	798 km
Band (wavelength)	C-band (5.6 cm)
Revisit cycle	24days
Spatial resolution	30 m
Incidence angle (°)	27.8
Polarization	VV
Centre Location	40.20 116.40
Number of images	72
Temporal coverage	2013/02/09–2020/11/28

were also studied. The remotely sensed measurements, levelling, extensometer data and groundwater level data have been gathered, and the dataset has been revised in the following paragraphs.

### 3.1.1 Remotely sensed data

PSI technique outcomes were obtained by processing Radarsat-2 acquisitions. A total of 68 Radarsat-2 images with 30-m resolution and 24-day revisit time acquired in Stripmap mode from February 2013 to November 2020 were processed. These stacks of Synthetic Aperture Radar (SAR) images were used to map land subsidence over the period from 2013 to 2020, respectively. The acquisition parameters of SAR images are presented in Table 1.

### 3.1.2 *In-situ* deformation data

The different-depth extensometers in Wangsiying land subsidence monitoring station and twenty levelling benchmarks were selected. The levelling results were used to calibrate and validate the land movements derived from PSI. The extensometer data recorded from 2006 to 2020 were selected to analyze the main subsidence contribution layer and the relationship between layered soil deformation and groundwater level. The monitoring layers of extensometers and groundwater wells in Wangsiying station are shown in Table 2. The location of Wangsiying station is shown in Figure 1.

### 3.1.3 Groundwater level data

The comparative maps of the groundwater level of different aquifer groups along the Beijing-Tianjin high-speed railway from 2015 to 2020 were drawn by virtue of the contour data of regional groundwater level in 2015 and 2020. In addition, time series analysis was conducted using data from 10 groundwater level observation wells in Wangsiying station and along the railway. D1-1, D1-2, D-3, D-4, and D1-5 wells are located in the Wangsiying land subsidence monitoring station. The monitoring layers are shown in Table 2. The aquifer group is a multi-layer structure composed of sand and cohesive soil, and the depths of the wells are 185 m, 155 m,

102 m, 54 m, and 19 m, respectively. Well 01, Well 02, Well 03, and Well 04 are located near the Beijing-Tianjin high-speed railway in the southeast of the plain. The lithology is mainly medium fine sand, and the depths of the wells are 182 m, 300 m, 166 m, and 300 m, respectively. The location of the Wangsiying station and the groundwater wells (Number: 01–04) are shown in Figure 1. The groundwater flow field and groundwater level variation process along the Beijing Tianjin high-speed railway were analyzed by the groundwater level monitoring data.

## 3.2 Methodologies

In this paper, the time-series InSAR monitoring data, *in situ* monitoring data of recent 20 years (such as groundwater level data, groundwater exploitation data and extensometer data) and a variety of basic geological data sets were combined to compare and analyze the changes of groundwater level, land subsidence and the main subsidence layers along the Beijing-Tianjin high-speed Railway before and after the SNWDP-CR. The effects of the environment of Quaternary sedimentary, groundwater exploitation and soil deformation of different lithology on land subsidence along the high-speed railway under the background of new water conditions were studied. Firstly, Radarsat-2 images, by means of PSI technique, are processed to obtain the long-term sequence of land subsidence distribution characteristics along the Beijing-Tianjin high-speed railway. The changes in land subsidence along the railway before and after the SNWDP-CR were analyzed. Secondly, the extensometer data from 2006 to 2019 in Wangsiying land subsidence monitoring station, the subsidence proportion of different compression layers along the railway was analyzed, and the main subsidence layers were identified. Thirdly, the regional groundwater level contour data were utilized to draw the comparative map of the groundwater level of different aquifer groups along the Beijing-Tianjin high-speed railway from 2015 to 2020. By combining the data of multiple groundwater wells, the changes in the groundwater flow field and groundwater level before and after the SNWDP-CR operation were analyzed by means of GIS and mathematical statistics methods. Fourthly, the effects of the environment of Quaternary sedimentary, groundwater exploitation and soil deformation with different lithology on land subsidence along the high-speed railway under the background of new water conditions were studied by comprehensively analyzed of the monitoring results of land subsidence and basic geological data set. The overall technical framework is shown in Figure 3.

### 3.2.1 PSI technique

The PSI technique mainly selects those pixels that maintain high coherence in the long-term sequence of SAR images as research objects, and the long-term sequence stability of them enables the accurate phase information to be obtained. By separating the phase of each coherent target point, including the elevation, the orbit, and the phase change of the atmosphere, the surface deformation can be obtained. This method can effectively overcome the influence of spatiotemporal descorrelation and atmospheric delay of DInSAR, and improve the monitoring accuracy of surface deformation up to millimeter level. PSI technology was originally developed by Ferretti (Ferretti and Prati, 2000; Ferretti et al., 2001)

TABLE 2 The monitoring layers of extensometers and groundwater wells in Wangsiying station.

Extensometers	F1-1	F1-2	F1-3	F1-4	F1-5	F1-6	F1-7
Monitoring depth (m)	147.5	94.0	66.0	50.0	24.0	15.0	2.0
Groundwater wells	D1-1	D1-2	D1-3	D1-4	D1-5	---	---
Monitoring depth (m)	161–182	124–147	66–94	24–46	9–14	---	---

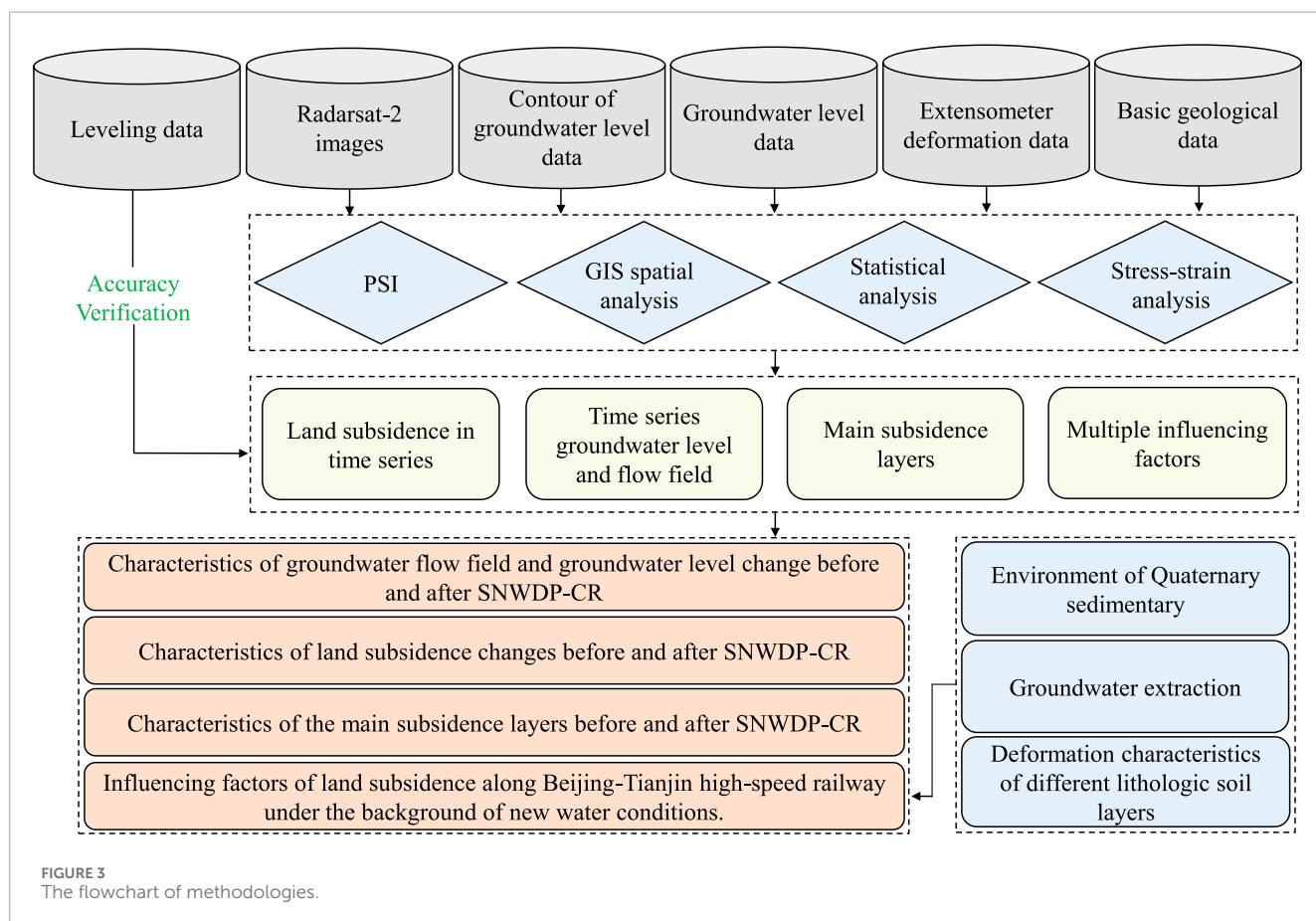


FIGURE 3 The flowchart of methodologies.

and since then it has been widely used in surface deformation monitoring (Galloway et al., 1998; Strozzi and Wegmuller, 1999; Hoffmann et al., 2001; Ng et al., 2012; Gong et al., 2018; Chen et al., 2020). The main steps in the PSI processing chain are as follows: selection of a master image from the available series of SAR scenes, construction of a series of interferograms, selection of permanent scatterers (PS) of the radar signal according to amplitude dispersion index and coherence thresholds, and phase unwrapping. The differential interferometric phase  $\Phi_{PS}$  of each PS in the interferogram can be expressed as the accumulation of five components (Hooper et al., 2004):

$$\Phi_{PS} = \Phi_{def} + \Phi_{top} + \Phi_{atm} + \Phi_{orb} + \Phi_n \quad (1)$$

In the formula (1),  $\Phi_{def}$  is the deformation phase along the line of sight,  $\Phi_{top}$  the topographic phase,  $\Phi_{atm}$  the phase component due to atmospheric delay,  $\Phi_{orb}$  the orbital error phase, and  $\Phi_n$  the phase

noise. The deformation phase  $\Phi_{def}$  of PS can be separated from the other components. An external DEM with resolution of 30 m is used to remove  $\Phi_{top}$  from the interferometric phase. The phases due to atmosphere delay and noise are removed through filtering processes (Teatini et al., 2007).

### 3.2.2 GIS spatial analysis and stress–strain analysis

The GIS spatial analysis method was used to compile the groundwater level comparison map of different aquifer groups along the Beijing–Tianjin high-speed railway in 2015 and 2020. Combining the data of multiple groundwater wells, the characteristics of groundwater flow field and the changes of groundwater level before and after SNWDP-CR were analyzed. In addition, GIS spatial analysis method was used to overlay and analyze the distribution of land subsidence and geological conditions on the Beijing–Tianjin high-speed railway. The

TABLE 3 Calibration of the displacements measured by PSI using leveling records.

Benchmark number	Average vertical movement by PSI (mm/yr)	Average vertical movement by leveling (mm/yr)	Difference (mm/yr)	Benchmark number	Average vertical movement by PSI (mm/yr)	Average vertical movement by leveling (mm/yr)	Difference (mm/yr)
S01	-38.5	-36.4	-2.1	S11	-15.6	-9.8	-5.8
S02	-30	-25	-5	S12	-29	-20	-9
S03	-36.2	-30.9	-5.3	S13	-14.2	-5.9	-8.3
S04	-19	-13	-6	S14	-17.6	-10.5	-7.1
S05	-20.8	-15.2	-5.6	S15	-38.4	-29.8	-8.6
S06	-30.2	-23.8	-6.4	S16	-28.6	-22.3	-6.3
S07	-36.5	-45.7	9.2	S17	-26.3	-18.6	-7.7
S08	-17.6	-22.6	5	S18	-19.8	-24.1	4.3
S09	-16.5	-10.6	-5.9	S19	-45	-47	2
S10	-13.6	-22.3	8.7	S20	-10.2	-16.2	6

Mean square error (mm/yr) 6.52.

stress-strain analysis method was used to study the deformation characteristics of the cohesive soil layers along the railway under the different groundwater level change mode before and after SNWDP-CR.

## 4 Results

### 4.1 Change of land subsidence

The outcomes of the PSI were calibrated by virtue of the twenty levelling benchmarks shown in Figure 1 and the calibration was carried out by using the average annual displacement rates over the period of investigation. Because of the lack of PS at the benchmarks, the average movement of the radar targets in a 100 m buffer zone around the levelling points was used as PSI value in the calibration procedure. The difference range of them is from 2 mm to 10 mm, with the mean square error being 6.52 mm (Table 3).

The time series land subsidence along the Beijing-Tianjin high-railway from 2013 to 2020 is shown in Figure 4. The Beijing-Tianjin high-speed railway (Beijing section) is approximately 50 km long and passes through the edge of Taihu subsidence funnel in Tongzhou District. From 2013 to 2020, the land subsidence rate in the Taihu area showed a slowing trend. The maximum subsidence rate decreased from 120 mm/yr in 2013 to 69 mm/yr in 2020. The section with severe land subsidence along the Beijing-Tianjin high-speed railway is from DK11 to DK23, with a length of approximately 12 km. From 2013 to 2020, the land subsidence along the railway also showed a slowing trend. The maximum subsidence rate along the Beijing-Tianjin high-speed railway reached 80 mm/yr from 2013 to 2016. Since 2017, the rate of

land subsidence along the railway has slowed down. The maximum subsidence rate decreased from 78 mm/yr in 2017 to 49 mm/yr in 2020.

From 2013 to 2020, the length of the section with a subsidence rate of 30–50 mm/yr along the Beijing-Tianjin high-speed railway decreased from 6.1 km to 3.9 km, and the length of the section with a subsidence rate greater than 50 mm/yr decreased from 8.0 km to 0 km (Table 4). Based on the rate of land subsidence over the years, the subsidence along the railway can be divided into three levels. 1) Areas with minor land subsidence. The subsidence rate of this section is 0–30 mm/yr, with an average length of 39.2 km. The subsidence slope changes gently, and the expected corner loss is relatively small. 2) Areas with moderate land subsidence. The subsidence rate of this section is 30–50 mm/yr, with an average length of 5.3 km. The change in subsidence slope has increased, and it is expected to cause significant corner loss. 3) Areas with intense land subsidence. The subsidence rate of this section is greater than 50 mm/yr, with an average length of 5.5 km. The uneven subsidence is significant, resulting in significant changes in subsidence slope and expected to cause significant corner loss (Figure 5). At present, the maximum subsidence slope change along the Beijing-Tianjin high-speed railway is 0.42‰, which is still within the allowable range (allowable value < 20‰). In addition, in some sections with severe subsidence, the track elevation has been adjusted to compensate for elevation loss, and speed reduction measures have been taken to ensure the safe operation of the railway. The corner loss is calculated as follows:  $T = R \tan(A/2)$ , where  $T$  is the tangent length;  $R$  is the radius of circular curve;  $A$  is the corner loss. The subsidence slope is calculated as follows:  $i = h/l \times 100\%$ , where  $i$  is the subsidence slope;  $h$  is the difference of elevation;  $l$  is the horizontal distance.

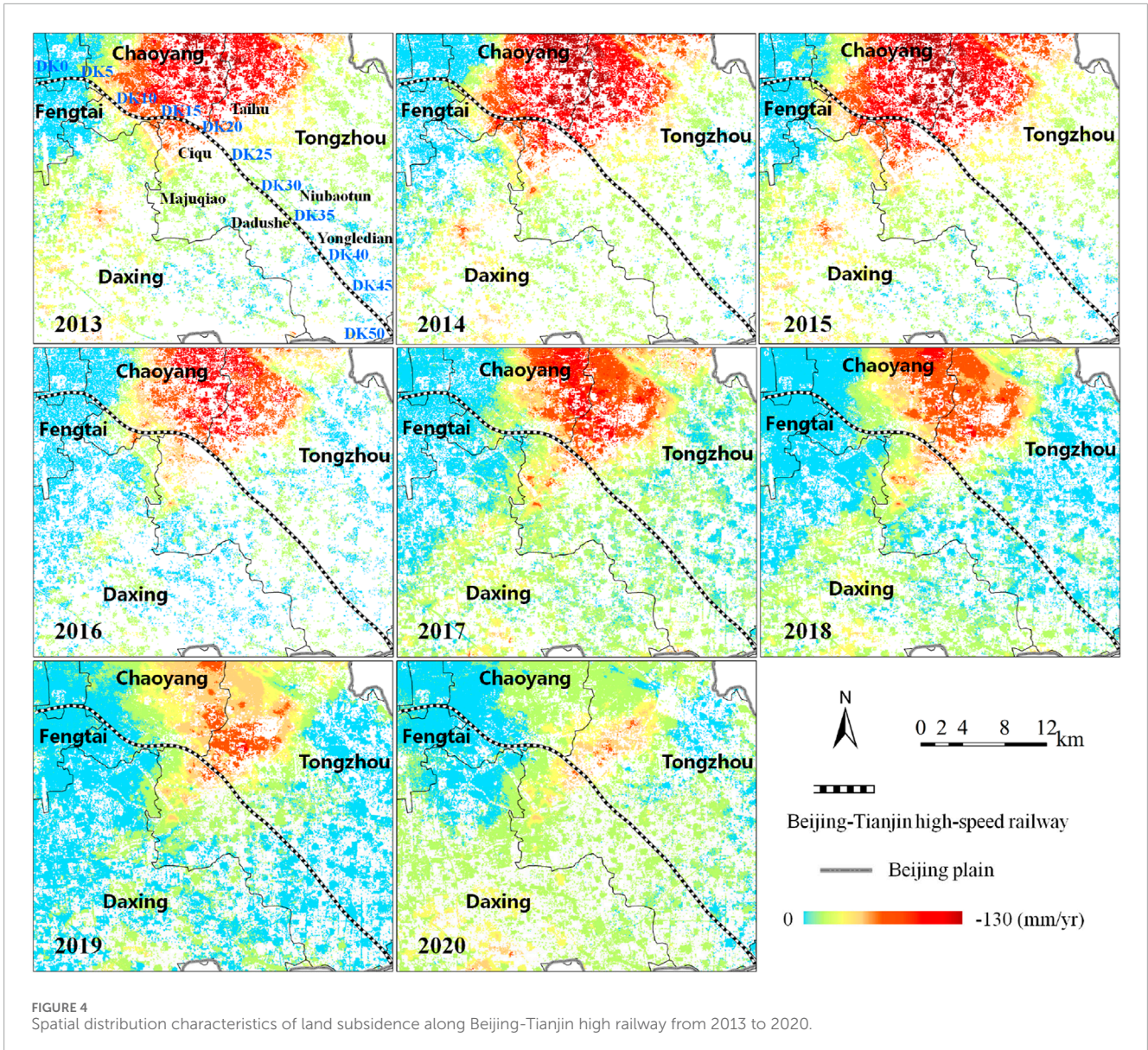


TABLE 4 Statistics of different subsidence rate and lengths along the Beijing-Tianjin high-speed railway from 2013 to 2020 (Unit: km).

Subsidence rate(mm/yr)	2013	2014	2015	2016	2017	2018	2019	2020	Average
0–30	35.9	35.4	34.8	40.2	40.2	39.1	42.5	46.1	39.2
30–50	6.1	5.7	7.0	4.6	4.2	5.1	5.4	3.9	5.3
>50	8.0	9.0	8.3	5.2	5.6	5.8	2.1	0.0	5.5

## 4.2 Change of subsidence at different depths

The extensometer monitoring data from 2006 to 2019 of Wangsiying land subsidence monitoring station along the Beijing Tianjin high-speed railway was used to analyze the deformation characteristics of soil layers at different depths and the main

contributing layers of land subsidence was identified. The total subsidence of Wangsiying station from 2006 to 2019 was 589.79 mm. The subsidence of the F1-1 and F1-2 extensometers is large, with corresponding monitoring layers of 148–182 m and 94–148 m, respectively. The subsidence of these two layers accounts for 21.82% and 47.18% of the total subsidence. From the perspective of each compression layer group, the subsidence proportions of the first,

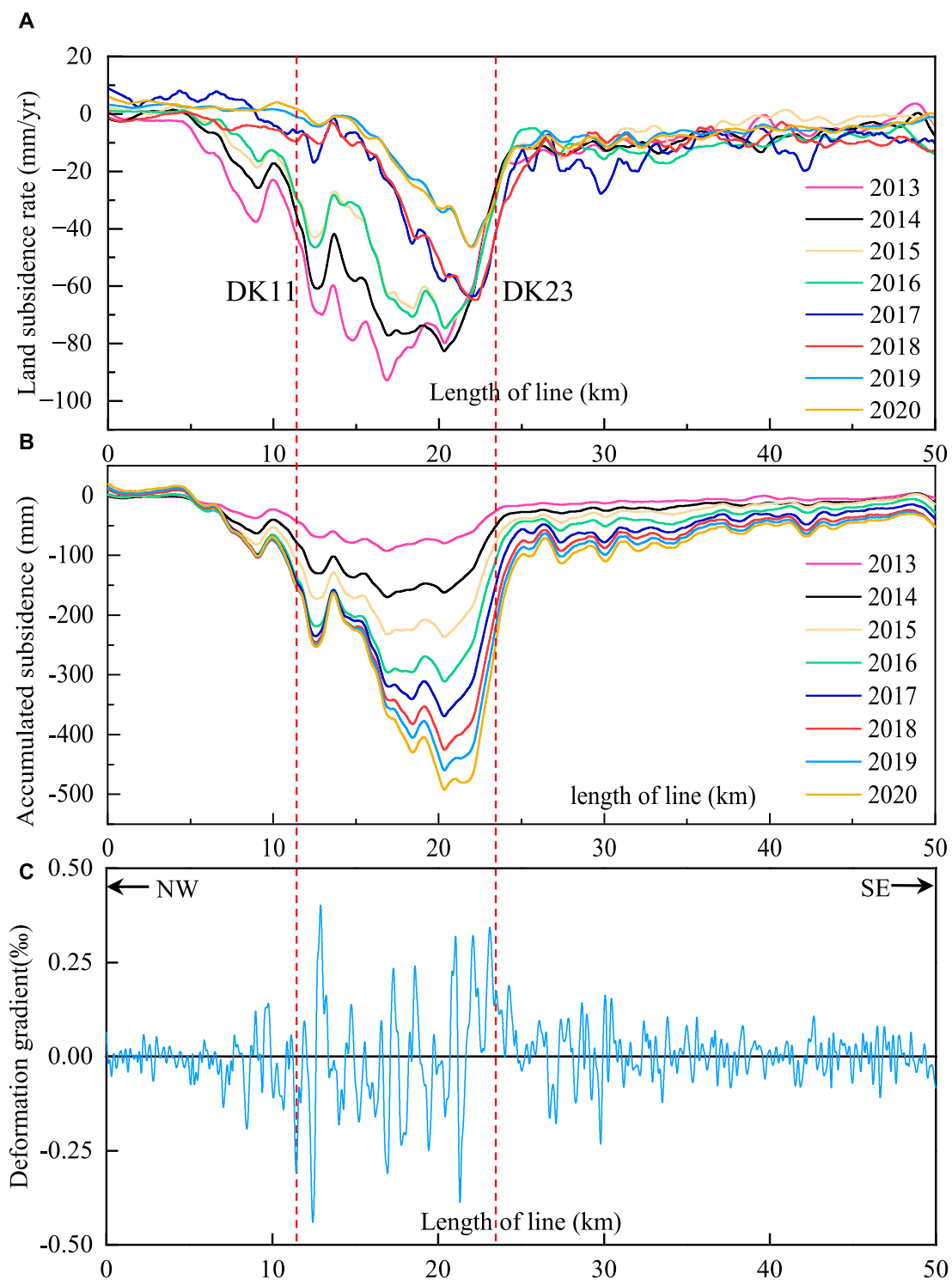
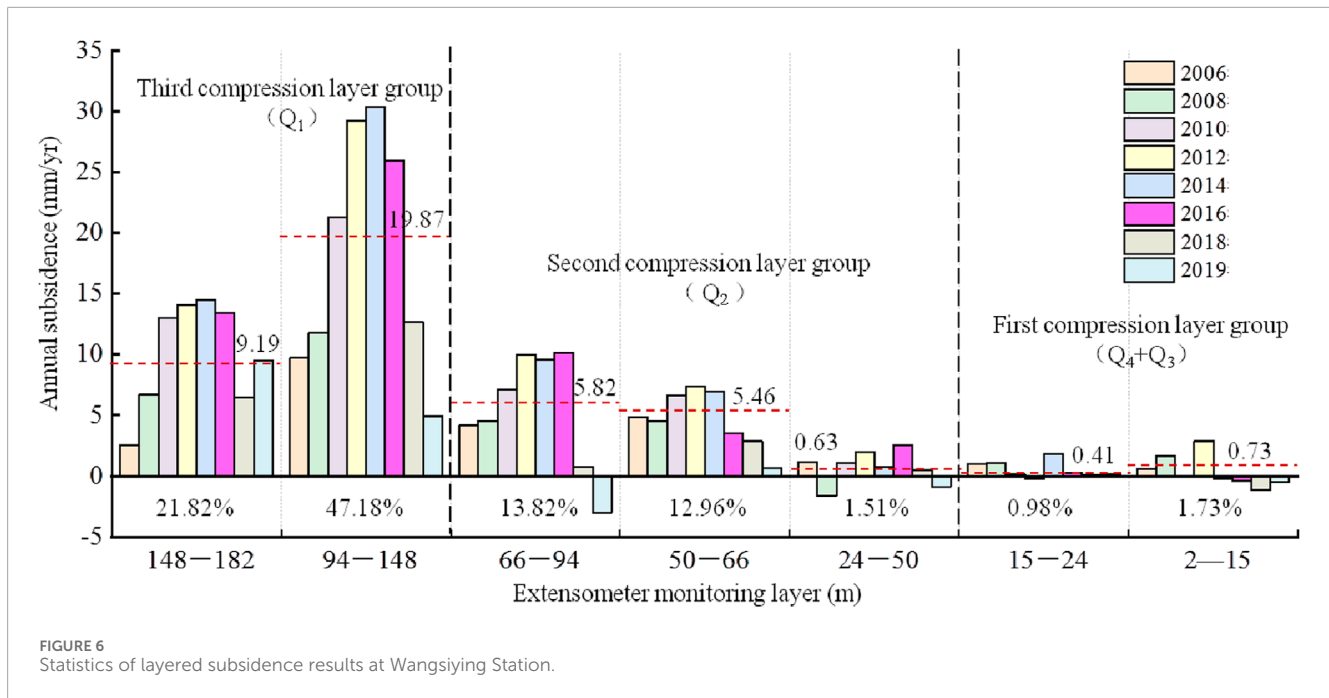


**FIGURE 5**  
The rate of subsidence, cumulative subsidence and the gradient of subsidence profile chart along Beijing-Tianjin high-speed railway from 2013 to 2020. (A) Land subsidence rate profile chart from 2013 to 2020. (B) Accumulated land subsidence profile chart from 2013 to 2020. (C) Land subsidence gradient profile chart from 2013 to 2020.

second, and third compression layer groups are 2.71%, 28.29%, and 69%, respectively. Among them, the third compressive layer group (94–182 m) has the largest subsidence proportion and is the main contributing layer to the subsidence (Figure 6). In addition,

according to the changes in the proportion of subsidence over the years at around 100 m of Wangsiying land subsidence monitoring station, it can be seen that the proportion of subsidence above 100 m of strata is relatively small, while the below 100 m of strata is



relatively large, and the proportion of deep strata subsidence shows an increasing trend (Figure 7B). The lithology of the Wangsiying monitoring station along the Beijing-Tianjin high-speed railway mainly includes silt, cohesive soil, fine sand, medium coarse sand, and coarse sand with gravel. According to the statistical results of lithology at different depths, the thickness of the cohesive soil in the third compressive layer group (94–182 m) is 54 m, accounting for 55% of the total thickness of the formation in this section (Figure 7A). It can be said that the thick cohesive soil layer provides an important material foundation for the compression of the strata in this section.

### 4.3 Change of groundwater level

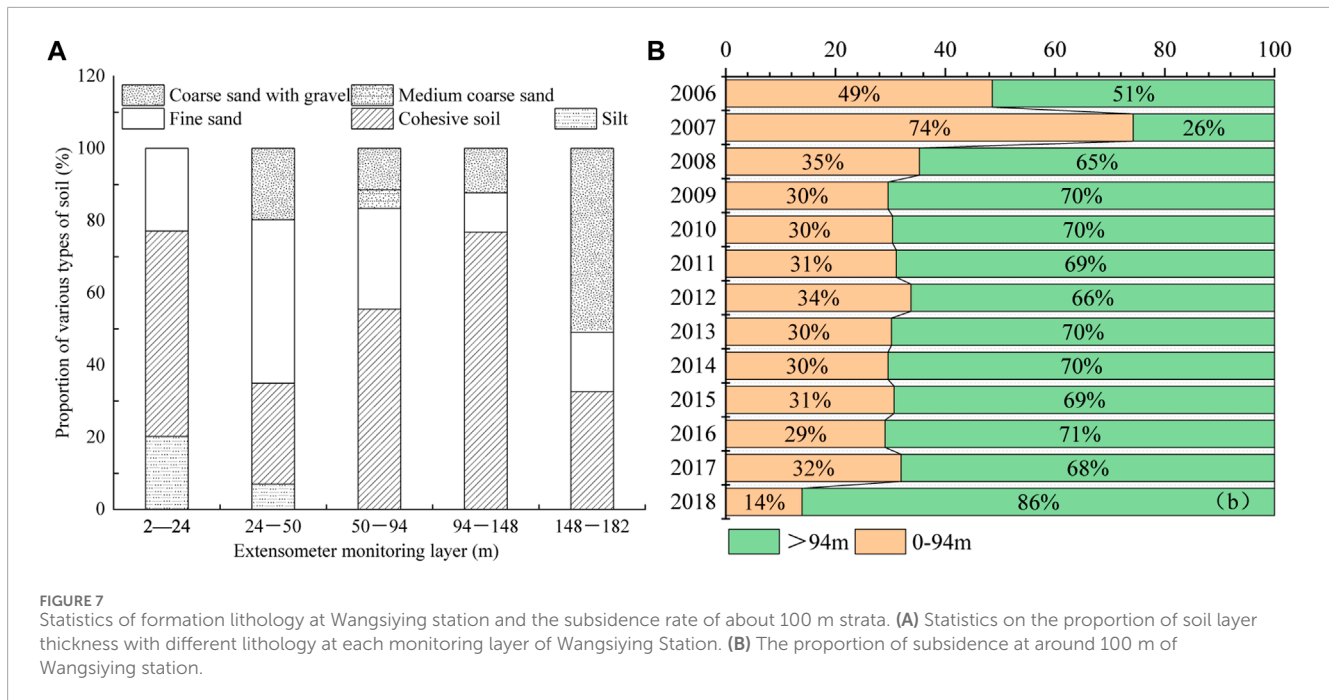
The monitoring data of groundwater level in 2015 and 2020 were used to draw a comparison map of groundwater level in different aquifer groups along the Beijing-Tianjin high-speed railway (Figure 8). It can be observed that after the SNWDP-CR, the groundwater level of different aquifer groups along the railway was still decreasing in some areas, but there were also some areas where the groundwater level rose. From 2015 to 2020, the phreatic water level of sections DK0-DK18 and DK43-DK50 along the Beijing-Tianjin high-speed railway showed an rise trend, while the other sections declined (Figure 8A). The groundwater level of the first confined aquifer group along the DK5-DK18 section of the railway showed an rise trend, while the other sections declined (Figure 8B). The groundwater level of the second confined aquifer group along the DK7-DK23 section of the railway showed an rise trend, while the other sections declined (Figure 8C). The groundwater level of the third confined aquifer group along the DK16-DK28 section of the railway showed an rise trend, while the other sections declined (Figure 8D).

According to the data from the groundwater level monitoring wells D1-1 to D1-5 at Wangsiying station, before 2017, the groundwater level of each aquifer group showed a continuous decline trend, with an average annual decline of 0.13–1.82 m. After 2017, the groundwater level of each aquifer group changed from decline to rise, with an average annual rise of 0.45–1.87 m (Figure 9A). According to the data from monitoring wells 01–04 along Beijing-Tianjin high-speed railway, the groundwater level in the southeastern region of the plain showed a continuous decline trend. From 2010 to 2020, the middle-deep and deep confined groundwater level continued to decline, with an average annual decreased of 1.2–1.8 m and a maximum cumulative decreased of over 19 m (Figure 9B). This showed that groundwater was still overexploited in some areas along the Beijing-Tianjin high-speed railway.

## 5 Discussion

### 5.1 Impact of quaternary sedimentary environment on land subsidence

The spatial distribution of land subsidence along the Beijing-Tianjin high-speed railway (Beijing section) shows significant differences, and the boundaries of some subsidence areas are located exactly at the structural boundary. The main structures include the Nanyuan-Tongxian fault, Xiadian-Mafang fault, Daxing uplift and Gu'an-Wuqing depression. As shown in Figure 10A. The variation of basement tectonic movement along the railway has affected the changes of Quaternary sedimentary environment to some extent, which is mainly reflected in the obvious differences in the thickness and lithology of Quaternary sediments. The Quaternary sedimentary environment along the Beijing-Tianjin high-speed railway can be divided into three parts. 1) Northwest



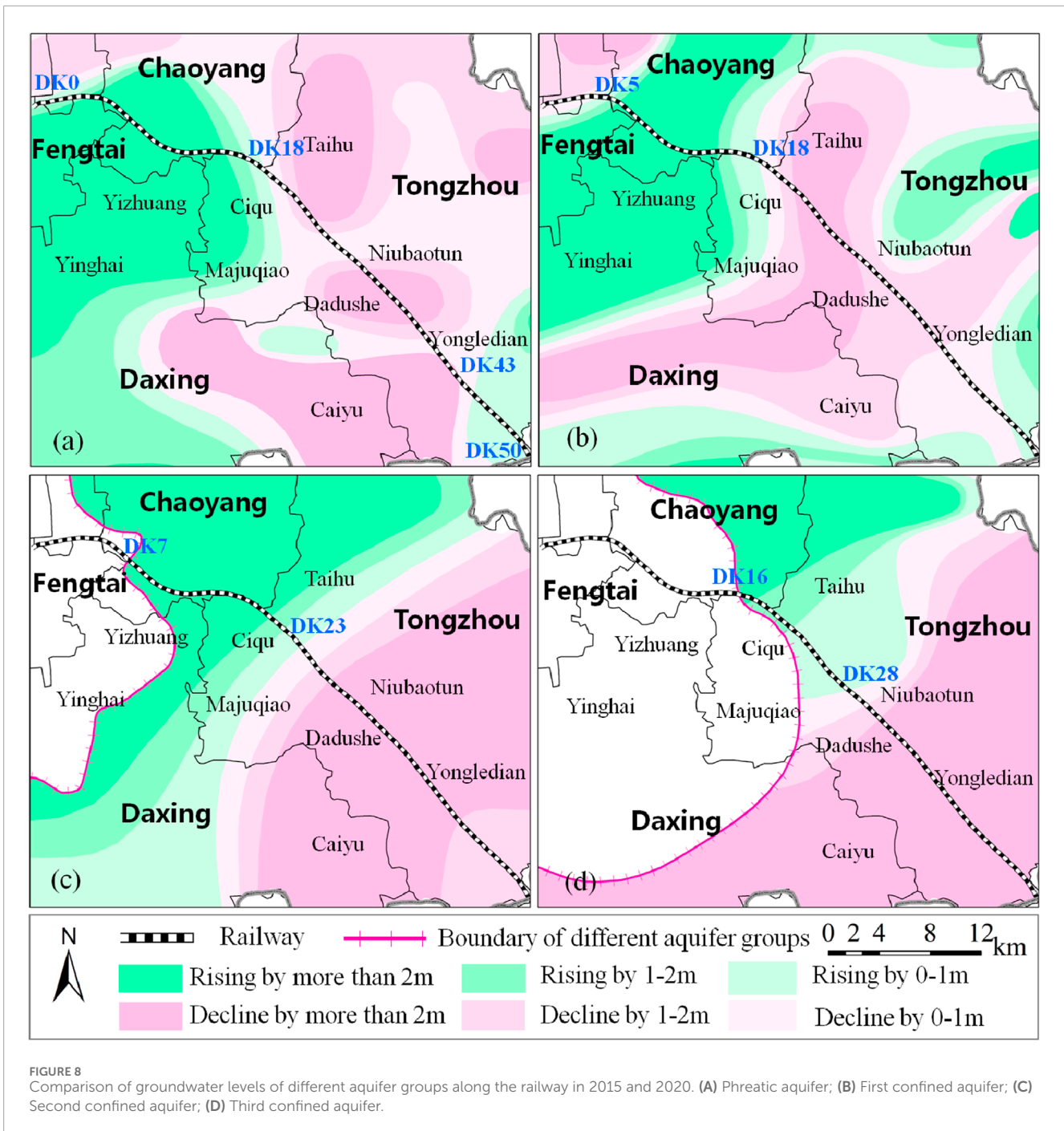
area of Nanyuan-Tongxian fault (DK0-DK7). This area was sunk during the Neogene period and covered with thicker Neogene strata on top of the Paleogene strata. However, during the Quaternary period, the area was relatively uplifted, and the Quaternary sediment thickness was less than 100 m. 2) Nanyuan-Tongxian fault to the Daxing uplift (DK7-DK25). The thickness of Quaternary sediments in the southeastern part of the Nanyuan-Tongxian fault increased gradually, but was partially affected by the Daxing uplift, and the thickness of quaternary sediments was thinner than that in Yongledian area (DK35-DK50) in Tongzhou District, with an average thickness of about 200 m. 3) Southeastern area of Daxing uplift (DK25-DK50). The area is located in the Dachang depression and the Gu'an-Wuqing depression, and received thicker sediments during the Quaternary period. The thickness of the Quaternary along the high-speed railway exceeds 300 m (Figure 2).

In addition, the Beijing-Tianjin high-speed railway (Beijing section) passes through the Yongding River alluvial fan and alluvial plain. The thickness of the Quaternary gradually increased from northwest to southeast, with more layers and the sediment particles also changed from coarse to fine. The proportion of cohesive soil is gradually increasing. In the northwest area of Nanyuan-Tongxian fault (DK0-DK7), the thickness of Quaternary is thin, the lithology is mainly coarse sand and gravel. The thickness of compressible cohesive soil layer is also relatively thin, and the land subsidence is not easy to occur. However, in the area from the Nanyuan-Tongxian fault to the Daxing uplift, the thickness of the Quaternary gradually increased, and the lithology gradually changed to an interlayer structure of sand and cohesive soil. The thickness of compressible cohesive soil layer gradually increased (Figure 10A). In addition, the continuous overexploitation of deep groundwater in this area that has led to serious land subsidence. For example, in section DK7-DK23

along the Beijing-Tianjin high-speed railway, the land subsidence is relatively severe, and the thickness of the compressible cohesive soil layer in this section is generally 80–120 m (Figure 10B). However, the land subsidence rate in section DK23-DK50 of the railway showed a slowing trend. This is mainly because the Quaternary sedimentation environment provides an important material foundation for the development of land subsidence, but the land subsidence is also affected by groundwater exploitation and human engineering activities, which can lead to obvious differences in spatial distribution of land subsidence along the Beijing-Tianjin high-speed railway.

## 5.2 Impact of groundwater exploitation on land subsidence

The problem of groundwater overexploitation along Beijing-Tianjin high-speed railway (Beijing section) is obvious. In the areas of severe land subsidence (DK7-DK23), the groundwater is mainly exploited for domestic and industrial purposes. In areas of small land subsidence (DK23-DK50), the groundwater is mainly exploited for agriculture. The exploitation of groundwater has caused a significant decline in the regional groundwater level (Figure 8) and has led to serious land subsidence (Figure 4). The results of land subsidence monitoring show that the spatial distribution difference of land subsidence along the Beijing-Tianjin high-speed railway is obvious. Most of the areas with severe land subsidence are located in the areas with severe groundwater overexploitation. Figure 11 shows that the subsidence of the railway (DK7-DK23) is relatively severe, and this section is the area with relatively high groundwater exploitation intensity. The intensity of groundwater exploitation in this section is greater than 1.1 million m<sup>3</sup>/km<sup>2</sup>. This indicates that the difference in groundwater exploitation



intensity is another major influencing factor for uneven subsidence along the Beijing-Tianjin high-speed railway. Based on the logistic regression analysis of groundwater level and deformation at different depths in Wangsiying Station along the Beijing-Tianjin high-speed Railway from 2006 to 2016, it is found that there is an obvious correlation between them (Figure 12). The correlation coefficient between groundwater level and deformation of F1-3 (66–94 m) monitoring layer reached 0.85, and that of F1-2 (94–148 m) monitoring layer reached 0.96. The statistical results reflect the relationship between groundwater level and subsidence well, and

further prove the important impact of groundwater exploitation on land subsidence.

The land subsidence of DK0-DK7 section of Beijing-Tianjin high-speed railway is minor. As mentioned before, this section is located in the southwest of Nanyuan-Tongxian fault, and the thickness of Quaternary is thin, the sediment particles are coarse, and the soil compressibility is low. In addition, the groundwater in this area is easy to be replenished by precipitation and lateral runoff, and the groundwater level recovers quickly, so the land subsidence in this area is minor.

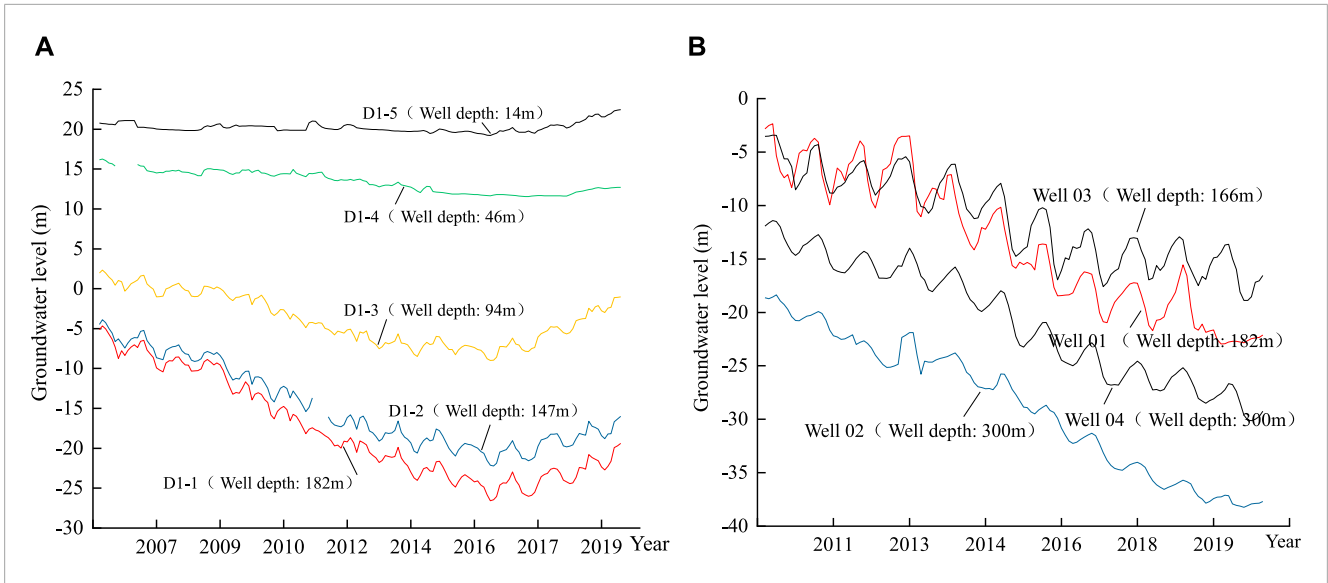


**FIGURE 9** Groundwater level change curves along the Beijing-Tianjin high-speed railway. (A) The groundwater level change curves of D1-1, D1-2, D-3, D-4 and D1-5 wells, which are located in the Wangsiying land subsidence monitoring station. (B) The groundwater level change curves of Well 01, Well 02, Well 03 and Well 04, which are located along the railway.

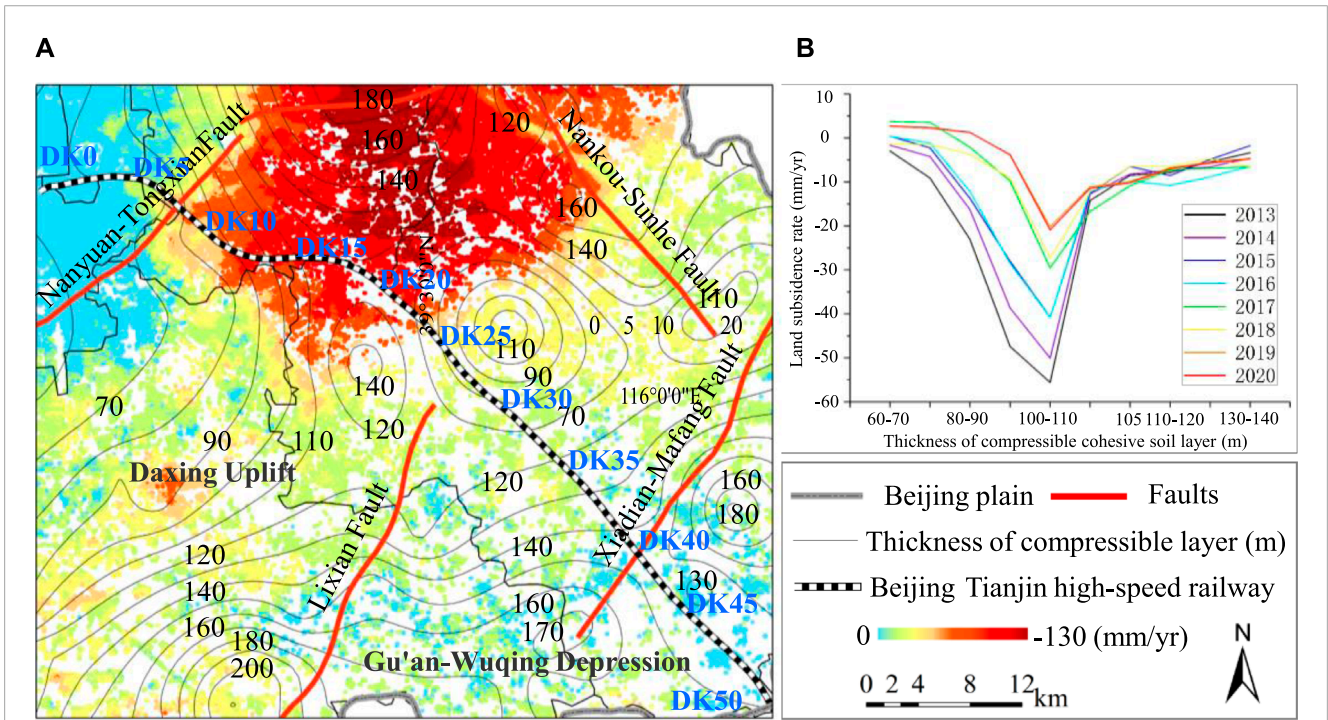


**FIGURE 10** Distribution of basement tectonic and thickness of compressible cohesive soil layer along the Beijing-Tianjin high-speed railway (Beijing section). (A) Basement tectonic and cohesive soil layer contour lines. (B) Statistics on the thickness of compressible cohesive soil layers of the areas with severe land subsidence from 2013 to 2020.

### 5.3 Impact of soil compression characteristics on land subsidence

In addition to the factors such as the Quaternary sedimentary environment and groundwater exploitation intensity, the

mechanical properties of soil layers with different depths and lithology are also factors affecting differential land subsidence along the Beijing-Tianjin high-speed railway (Beijing section). The whole line of Beijing-Tianjin high-speed railway adopts bored pile foundation to control land subsidence. The pile length of bridge

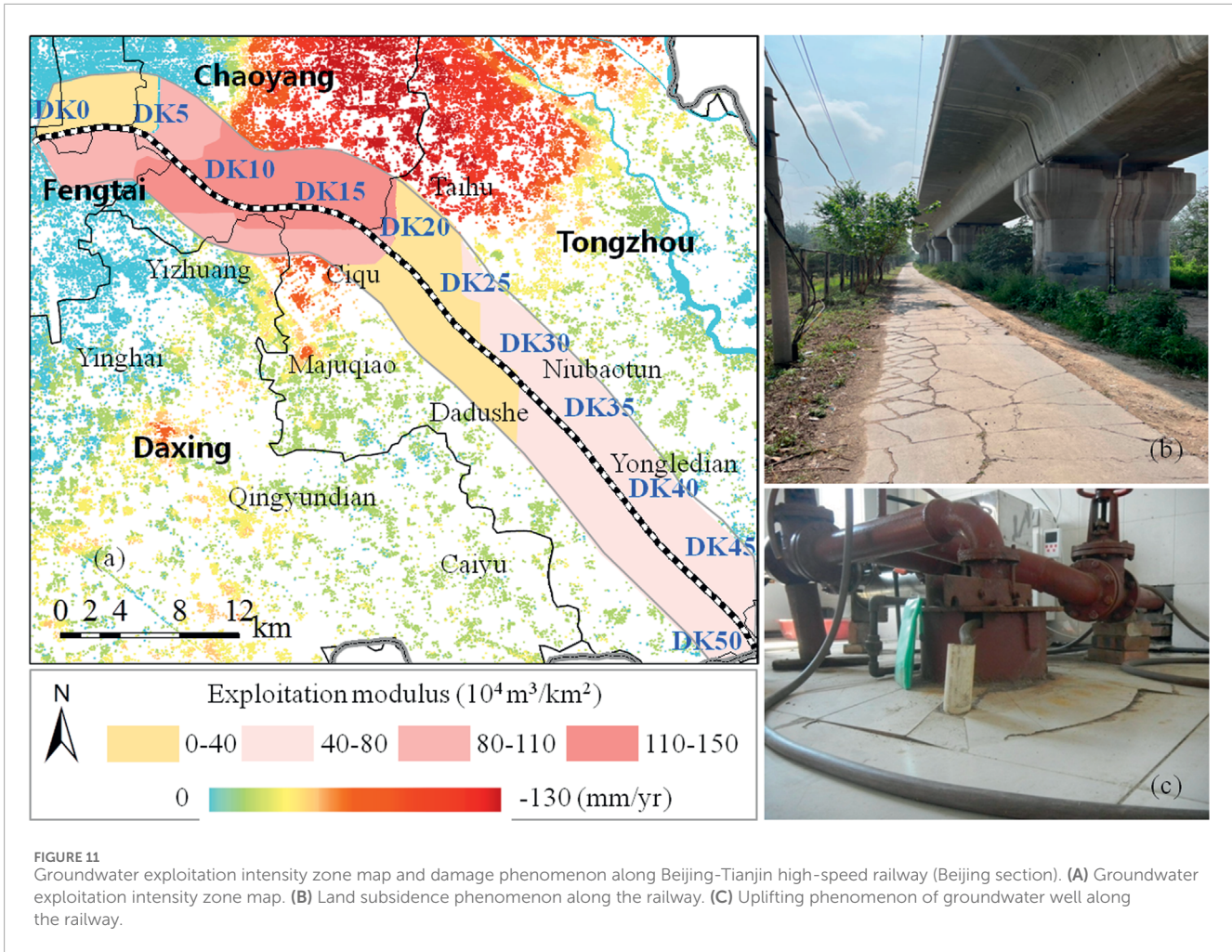


**FIGURE 11** Groundwater exploitation intensity zone map and damage phenomenon along Beijing-Tianjin high-speed railway (Beijing section). **(A)** Groundwater exploitation intensity zone map. **(B)** Land subsidence phenomenon along the railway. **(C)** Uplifting phenomenon of groundwater well along the railway.

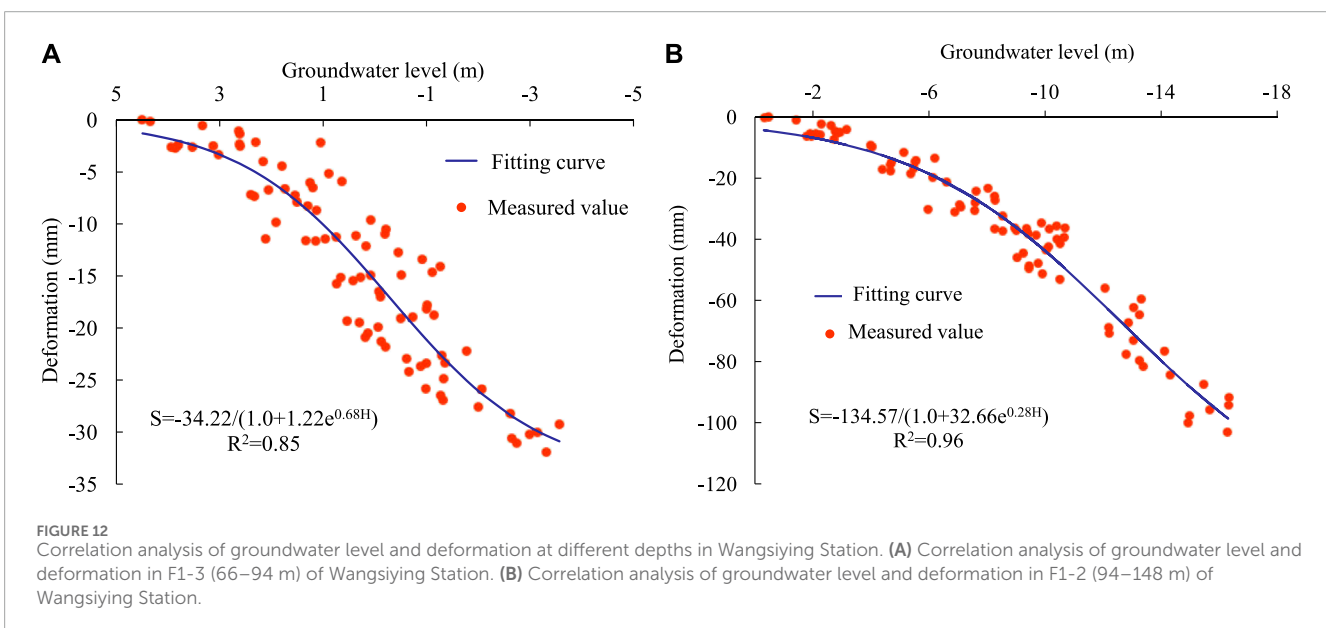
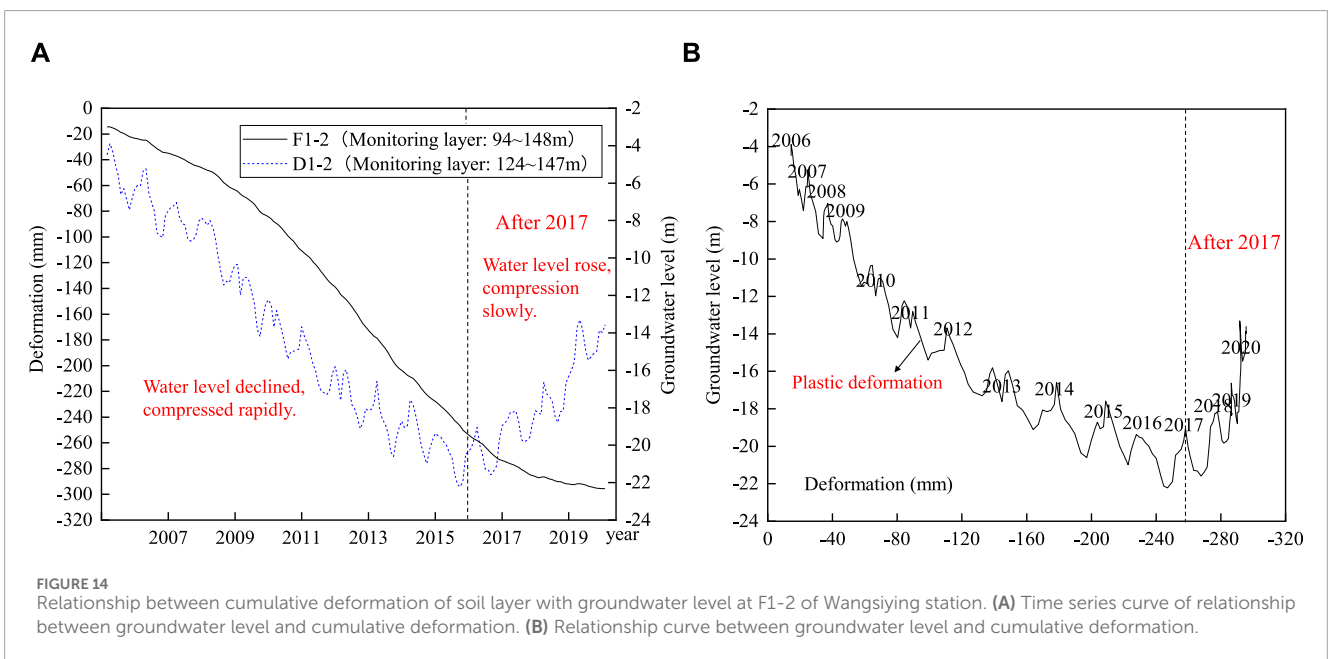
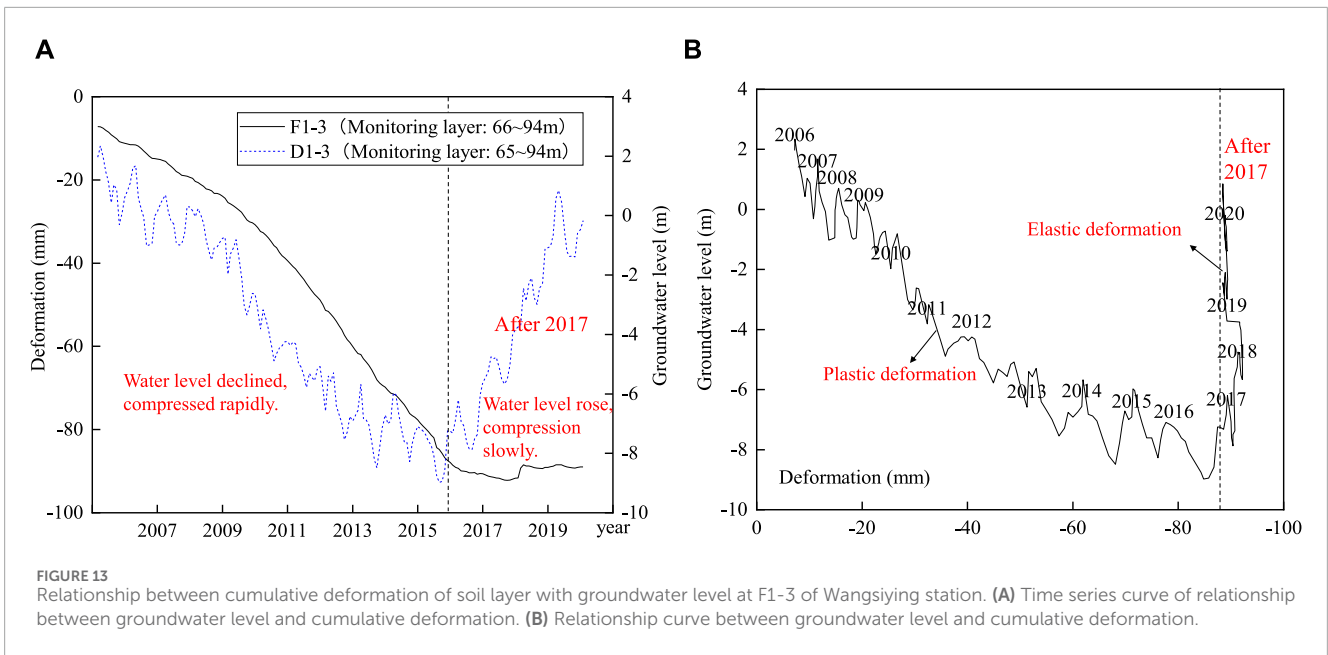


**FIGURE 12** Correlation analysis of groundwater level and deformation at different depths in Wangsiying Station. **(A)** Correlation analysis of groundwater level and deformation in F1-3 (66-94 m) of Wangsiying Station. **(B)** Correlation analysis of groundwater level and deformation in F1-2 (94-148 m) of Wangsiying Station.



is about 50m, and the pile length of long-span bridge is generally about 65 m. Therefore, the subsidence of strata above 50 m has little impact on high-speed railway. The strata which have great impact on the subsidence of high-speed railway are mainly concentrated in the strata below 50 m. Stress-strain analysis was carried out with the extensometer and groundwater level monitoring data by the strata below 50 m in Wangsiying station. The influence of soil deformation with different depth and lithology on Beijing-Tianjin high-speed railway (Beijing section) was analyzed.

The monitoring layer of extensometer F1-3 in Wangsiying station is 66–94m, with a total thickness of 28 m. It is mainly composed of clay layer and sand layer. The sand layer accounts for about 74% of the total thickness of the section, and the

clay layer 26%. As shown in [Figure 13A](#), from 2006 to 2016 the groundwater level showed an overall declined trend. Since 2017, the groundwater level has risen significantly. Before 2017, the groundwater level fluctuated periodically throughout the year. In each cycle, the groundwater level declined more than it rose. The effective stress on the soil layer increased, and the soil layer continued to compress rapidly. After 2017, the groundwater level rose significantly, the compression rate of the soil layer slowed down, and the soil layer rebounded slightly in 2019 and 2020. As shown in [Figure 13B](#), the monitoring layer was dominated by sand. From 2006 to 2016, with the decline of the groundwater level, the soil layer continued to compress rapidly, with a large amount of plastic deformation and with the phenomenon of hysteresis. This

TABLE 5 Deformation characteristics of different soil layers before and after SNWDP-CR operation under different groundwater level change modes.

Extensometer	Monitoring layer(m)	Groundwater level change modes	Deformation characteristics (groundwater level decline stage)	Deformation characteristics (groundwater level rise stage)
F1-3	66–94	The groundwater level decline continuously at first, and then gradually rise	The soil layer was compressed rapidly, with the residual deformation large. The soil layer was mainly plastic deformation, creep deformation included	1) When the soil layer was dominated by sand, the compression rate of the soil layer is significantly slowed down. The soil layer contained plastic deformation, creep deformation and elastic deformation. 2) When the soil layer was dominated by cohesive soil, the soil layer continued to compress, and the compression speed slowed down. The soil layer contained plastic deformation and creep deformation
F1-2	94–148			

was related to the fact that the dissipation of excess pore water pressure in the soil layer lagged behind the change of the aquifer water level, and it may also be related to the creep deformation. After 2017, when the local water level has risen significantly, the compression rate of the soil layer has slowed down, including plastic and creep deformation. There were elastic deformation occurred in 2019 and 2020. It can be seen that with the change of the groundwater level, the soil layer undergoes a process of changing from viscoplastic deformation to viscoelastic plastic. In addition, with the continuous water supply of the SNWDP-CR and groundwater exploitation reduction, the groundwater level in some areas along the Beijing-Tianjin high-speed railway may rise significantly in the future, which will further lead to the subsidence and rebound of the strata increased, and have a certain degree of impact on the safe operation of the high-speed railway, which needs further study.

The monitoring layer of extensometer F1-2 in Wangsiying station is 94–148 m, with a total thickness of 54 m. It is mainly composed of cohesive soil layer and sand layer, and the cohesive soil layer accounts for about 77% of the total thickness of this section. As shown in Figure 14A, from 2006 to 2016 the groundwater level showed a downward trend, and the soil layer continued to compress. After 2017, the groundwater level gradually rose, and the compression rate of the soil layer slowed down. As shown in Figure 14B, from 2006 to 2016 the extensometer F1-2 mainly exhibited plastic deformation and had a certain degree of hysteresis. From 2017 to 2020, the soil layer continued to compress during the rising stage of groundwater level, but the compression rate decreased. This showed that there was not only plastic deformation, but also creep deformation which related to the time development. It can be found that with the change of the groundwater level, the soil layer exhibits the characteristics of viscoplastic deformation. The deformation characteristics of the soil layers with different depths and lithology before and after the SNWDP-CR operation under different groundwater level change modes along the railway are shown in Table 5.

## 6 Conclusion

In this paper, the time-series InSAR monitoring data, *in situ* monitoring data of recent 20 years (such as groundwater level data, groundwater exploitation data and extensometer data) and a variety of basic geological data sets are combined to compare and analyze the changes of groundwater level, land subsidence and the main subsidence layers along the Beijing-Tianjin high-speed Railway before and after the SNWDP-CR. The effects of the environment of Quaternary sedimentary, groundwater exploitation and soil deformation of different lithology on land subsidence along the high-speed railway under the background of new water conditions are revealed. The main conclusions are as follows:

- (1) The PSI monitoring results showed that the serious land subsidence area along the Beijing-Tianjin high-speed railway always concentrated in section DK11-DK23 before and after the SNWDP-CR. After the operation of SNWDP-CR, the land subsidence along the railway generally showed a slowing trend. The maximum subsidence rate was reduced from 80 mm/yr to 49 mm/yr. The length of subsidence rate that more than 50 mm/yr of the section was reduced from 8.0 km to 0 km. The maximum subsidence gradient was 0.42%, which was still within the allowable range.
- (2) The groundwater level of different aquifer groups along the Beijing-Tianjin high-speed railway rose and declined before and after the SNWDP-CR. In eastern part of the plain, the groundwater level of each aquifer group has changed from a continuous decline (range 0.13–1.82 m) to a gradual rise (range 0.45–1.87 m) since 2017. However, in the southeast of the plain, the groundwater level still showed a continuous decline trend, with an average annual decline of 1.2–1.8 m. This suggested that the groundwater in these areas continued to be overexploited.
- (3) From 2006 to 2019, the subsidence of the first, second and third compression layer group along the railway accounted for 2.71%, 28.29% and 69%, respectively. The third compression

layer group (monitoring layer 94–182 m) had the largest subsidence proportion and was the main subsidence layer. In addition, the proportion of subsidence of deep strata at a depth of 100 m was about 70%, and the proportion changed slightly before and after the SNWDP-CR. But after 2018, the proportion showed an increasing trend.

- (4) The land subsidence along the Beijing-Tianjin high-speed railway was controlled by Nanyuan-Tongxian fault, Xiadian-Mafang fault, Daxing uplift and Gu'an-Wuqing depression. In addition, the difference of groundwater exploitation intensity led to differences in the spatial distribution of land subsidence along the railway. The subsidence of the soil layer below the bearing layer (about 50 m) of the high-speed railway pile foundation accounted for more than 97%. The cohesive soil layer in this section was relatively thick and mainly exhibited viscoplastic or viscoelastic plasticity deformation. This section of strata is a key layer that needs to be considered for land subsidence control along the Beijing-Tianjin high-speed railway. At the same time, the impact of land subsidence on bridges and tracks of Beijing-Tianjin high-speed railway, as well as the control of groundwater and the prevention measures of subsidence along the railway are all the issues that we need to strengthen research in future.

## Data availability statement

The original contributions presented in the study are included in the article/Supplementary material, further inquiries can be directed to the corresponding author.

## Author contributions

SL: Conceptualization, Data curation, Formal Analysis, Investigation, Methodology, Software, Writing—original draft,

Writing—review and editing. MB: Conceptualization, Data curation, Funding acquisition, Resources, Supervision, Validation, Writing—review and editing.

## Funding

The author(s) declare that financial support was received for the research, authorship, and/or publication of this article. This research is supported by the Natural Science Foundation of China (Grant No. 42172311).

## Acknowledgments

We greatly thank the editors, as well as the reviewers for their helpful or valuable comments on the paper.

## Conflict of interest

The authors declare that the research was conducted in the absence of any commercial or financial relationships that could be construed as a potential conflict of interest.

## Publisher's note

All claims expressed in this article are solely those of the authors and do not necessarily represent those of their affiliated organizations, or those of the publisher, the editors and the reviewers. Any product that may be evaluated in this article, or claim that may be made by its manufacturer, is not guaranteed or endorsed by the publisher.

## References

- Abidin, H., Andreas, H., Gumilar, I., and Brinkman, J. (2015). Study on the risk and impacts of land subsidence in Jakarta. *Proc. Int. Assoc. Hydrological Sci.* 372, 115–120. doi:10.5194/piahs-372-115-2015
- Bai, P., and Liu, C. (2018). Evolution law and attribution analysis of water utilization structure in Beijing. South-to-North Water Transf. *Water Sci. Technol.* 16 (4), 6. doi:10.13476/j.cnki.nsbqk.2018.0090
- Chen, B., Gong, H., Chen, Y., Lei, K., Zhou, C., Si, Y., et al. (2021). Investigating land subsidence and its causes along Beijing high-speed railway using multi-platform InSAR and a maximum entropy model. *Int. J. Appl. Earth Observation Geoinformation* 96, 102284. doi:10.1016/j.jag.2020.102284
- Chen, B., Gong, H., Chen, Y., Li, X., Zhou, C., Lei, K., et al. (2020). Land subsidence and its relation with groundwater aquifers in Beijing Plain of China. *Sci. Total. Environ.* 735, 139111. doi:10.1016/j.scitotenv.2020.139111
- Duan, G., Gong, H., Liu, H., Zhang, Y., Chen, B., and Lei, K. (2016). Monitoring and analysis of land subsidence along Beijing-tianjin inter-city railway. *J. Indian Soc. Remote Sens.* 44 (6), 915–931. doi:10.1007/s12524-016-0556-7
- Ferretti, A., Prati, C., and Rocca, F. (2000). Nonlinear subsidence rate estimation using permanent scatterers in differential SAR interferometry. *IEEE Trans. Geosci. Remote. Sens.* 38 (5), 2202–2212. doi:10.1109/36.868878
- Ferretti, A., Prati, C., and Rocca, F. (2001). Permanent scatterers in SAR interferometry. *Ieee. Trans. Geosci. Remote. Sens.* 39 (1), 8–20. doi:10.1109/36.898661
- Galloway, D., Hudnut, K., Ingebritsen, S., Phillips, S., Peltzer, G., Rogez, F., et al. (1998). Detection of aquifer system compaction and land subsidence using interferometric synthetic aperture radar, Antelope Valley, Mojave Desert, California. *Water. Resour. Res.* 34 (10), 2573–2585. doi:10.1029/98wr01285
- Ge, L., Li, X., Chang, H., Ng, A., and Hu, Z. (2010). Impact of ground subsidence on the Beijing-Tianjin high-speed railway as mapped by radar interferometry. *Ann. Gis Geogr. Inf. Sci.* 16 (2), 91–102. doi:10.1080/19475683.2010.492125
- Gong, H., Pan, Y., Zheng, L., Li, X., Zhu, L., Zhang, C., et al. (2018). Long-term groundwater storage changes and land subsidence development in the North China Plain (1971–2015). *Hydrogeol. J.* 26, 1417–1427. doi:10.1007/s10040-018-1768-4
- Helena, S., Oliveira, L., Henriques, M., Falco, A., Fonseca, J., Cooksley, G., et al. (2013). Persistent Scatterers Interferometry detects and measures ground subsidence in Lisbon. *Remote Sens. Environment* 115, 2152–2167. doi:10.1016/j.rse.2011.04.021
- Hoffmann, J., Zebker, H., Galloway, D., and Amelung, F. (2001). Seasonal subsidence and rebound in Las Vegas Valley, Nevada, observed by synthetic aperture radar interferometry. *Water. Resour. Res.* 37 (6), 1551–1566. doi:10.1029/2000wr900404
- Hooper, A., Zebker, H., Segall, P., and Kampes, B. (2004). A new method for measuring deformation on volcanoes and other natural terrains using InSAR persistent scatterers. *Geophys. Res. Lett.* 31, 1–5. doi:10.1029/2004gl021737
- Hu, X., Song, D., Wang, S., Li, Y., Sun, M., Zhong, S., et al. (2011). Analysis of correlation between groundwater exploitation and land subsidence in certain areas along Beijing-Shanghai high-speed railway. *Chin. J. Rock Mech. Eng.* 30 (9), 1738–1746. doi:10.1007/s12583-011-0163-z

- Hwang, C., Hung, W., and Liu, C. (2008). Results of geodetic and geotechnical monitoring of subsidence for Taiwan High Speed Rail operation. *Nat. Hazards* 47 (1), 1–16. doi:10.1007/s11069-007-9211-5
- Jiang, Y., Yang, M., Liao, M., and Wang, H. (2013). Deformation monitoring of the Shanghai Maglev system based on the time-series analysis of InSAR data. *Shanghai Land and Resour.* 34 (04), 17–20. doi:10.3969/j.issn.2095-1329.2013.04.005
- Kontogianni, V., Psimoulis, P., and Stiros, S. (2006). What is the contribution of time-dependent deformation in tunnel convergence. *Eng. Geol.* 82 (4), 264–267. doi:10.1016/j.enggeo.2005.11.001
- Lei, K., Luo, Y., Chen, B., Guo, G., and Zhou, Y. (2016). Distribution characteristics and influence factors of land subsidence in Beijing area. *Geol. China* 43 (6), 2216–2225. doi:10.12029/gc20160628
- Lei, K., Luo, Y., Liu, H., Tian, M., Wang, X., Kong, X., et al. (2020). *Land subsidence monitoring report of Beijing*. Beijing: Beijing Institute of Hydrogeology and Engineering Geology Beijing Institute of Geo-Environment Monitoring.
- Lei, K., Ma, F., Chen, B., Luo, Y., Cui, W., Zhao, L., et al. (2023). Effects of South-to-North water diversion project on groundwater and land subsidence in Beijing, China. *Bull. Eng. Geol. Environ.* 82, 18. doi:10.1007/s10064-022-03021-2
- Lei, K., Ma, F., Chen, B., Luo, Y., Cui, W., Zhou, Y., et al. (2022). Characteristics of land-subsidence evolution and soil deformation before and after the Water Diversion Project in Beijing, China. *Hydrogeology J.* 30, 1111–1134. doi:10.1007/s10040-022-02489-2
- Leng, C. (2011). Analysis of the factor and mechanism of uneven settlement of high-speed railway subgrade. *High. Speed Railw. Technol.* 2 (03), 5–8. doi:10.3969/j.issn.1674-8247.2011.03.002
- Li, G., Huang, D., and Gao, W. (2019). The analysis of ground subsidence along jakarta–bandung high-speed railway and main control measures. *Railw. Stand. Des.* 63 (02), 1–8. doi:10.13238/j.issn.1004-2954.201804250002
- Li, G., Zhang, J., Zhang, G., Sun, Z., and Xu, Z. (2007). The influence of pumping shallow groundwater on construction of high-speed railway and its countermeasures. *J. Railw. Eng. Soc.* 24 (12), 23–27. doi:10.3969/j.issn.2095-1329.2014.04.030
- Liu, H., Zhang, Y., Wang, R., Gong, H., Gu, Z., Kan, J., et al. (2016). Monitoring and analysis of land subsidence along the Beijing-Tianjin high-speed railway (Beijing section). *Chin. J. Geophys.* 59 (07), 2424–2432.
- Lu, Z., Chen, B., Gong, H., Zhou, C., Shi, M., and Cao, J. (2023). Evolution characteristics of land subsidence in Beijing section of beijing-tianjin intercity railway before and after the SouthSouth-to-North water diversion project. *Geomatics Inf. Sci. Wuhan Univ.* 48, 1959–1968. doi:10.13203/j.whugis20210214
- Ng, H., Ge, L., Li, X., and Zhang, K. (2012). Monitoring ground deformation in Beijing, China with persistent scatterer SAR interferometry. *J. Geod.* 86, 375–392. doi:10.1007/s00190-011-0525-4
- Shi, H., Liu, G., and Yang, S. (2014). Regional subsidence stability evaluation along Jingjin high-speed railway based on MT-InSAR. *J. Beijing Jiaot. Univ.* 38 (06), 78–81. doi:10.11860/j.issn.1673-0291.2014.06.014
- Shi, M., Chen, B., Gong, H., Li, X., Chen, W., Gao, M., et al. (2019). Monitoring differential subsidence along the beijing–tianjin intercity railway with multiband SAR data. *Int. J. Environ. Res. Public Health* 16, 4453. doi:10.3390/ijerph16224453
- Strozzi, T., and Wegmuller, U. (1999). Land subsidence in Mexico City mapped by ERS differential SAR interferometry. Geoscience and remote sensing symposium, IGARSS '99 proceedings. *IEEE Int. 4*, 1940–1942. doi:10.1109/igarss.1999.774993
- Sun, S., Zhang, W., Wang, Z., Su, W., Wu, C., and Bu, Q. (2009). Design of unballasted track bridges in beijing-tianjin inter-city railway. *Railw. Constr. Technol.* (02), 13–23. doi:10.3969/j.issn.1009-4539.2009.02.003
- Teatini, P., Strozzi, T., Tosi, L., Wegmüller, U., Werner, C., and Carbognin, L. (2007). Assessing short- and long-time displacements in the Venice coastland by synthetic aperture radar interferometric point target analysis. *J. Geophys. Res.* 112, F01012. doi:10.1029/2006jfo00656
- Wang, Q., Peng, J., Jiang, Z., and Teng, H. (2014). Numerical simulation and layerwise mark monitoring of land subsidence and ground fissures of typical section in Xi'an. *Rock Soil Mech.* 35 (11), 3298–3302. doi:10.16285/j.rsm.2014.11.016
- Yang, B., Liu, G., Yao, J., Li, Z., Feng, H., Mao, W., et al. (2020). Ground settlement monitoring and time-series evolution situation analyzing along high speed railway in beijing-tianjin-hebei region. *China Railw. Sci.* 41 (01), 1–9.
- Yang, H. (2013). Influence of high-speed-railway engineering works on groundwater drawdown and land subsidence on the Choushui River alluvial plain, Taiwan. *Shanghai Land and Resour.* 34 (4), 25–32. doi:10.3969/j.issn.2095-1329.2013.04.007
- Zhang, X., Chen, B., Lei, K., Chen, W., Gao, M., Zhou, C., et al. (2019). Characteristics of land subsidence along Beijing-Tianjin inter-city railway (Beijing section). *Remote Sens. Land and Resour.* 31 (01), 171–179. doi:10.6046/gtzyyq.2019.01.23
- Zhang, X., Ge, D., Xiao, B., Zhang, L., and Hou, M. (2014). Study on multi-track integration PS-InSAR monitoring the land subsidence along the highway—taking JingHu highway (Beijing-Hebei) as an example. *Bull. Surv. Mapp.* (10), 67–69. doi:10.13474/j.cnki.11-2246.2014.0331
- Zhang, Y. (1998). Introduction to Japan's high-speed railway subgrade treatment measures. *Railw. Stand. Des.* (12), 40–41. doi:10.3969/j.issn.1009-4539.2014.05.030
- Zhao, H., Liu, W., Sun, C., Jiao, Z., Li, M., Wang, S., et al. (2020b). *Beijing water resources bulletin*. Beijing: Beijing Water Authority.
- Zhao, X., Chen, B., Gong, H., Zhou, C., Li, X., Lei, K., et al. (2020a). Land subsidence along the beijing–tianjin intercity railway during the period of the SouthSouth-to-North water diversion project. *Int. J. Remote Sens.* 41 (12), 4447–4469. doi:10.1080/01431161.2020.1718238